Soft Matter

Mechanical properties of Staphylococcus aureus and Pseudomonas aeruginosa dual-species biofilms grown in chronic wound based models

Journal:	*Soft Matter*
Manuscript ID	SM-ART-12-2024-001441.R1
Article Type:	Paper
Date Submitted by the Author:	13-Feb-2025
Complete List of Authors:	Bhattarai, Bikash; Texas Tech University, Mechanical Engineering Christopher, Gordon; Texas Tech University, Mechanical Engineering

SCHOLARONE™
Manuscripts

Mechanical properties of *Staphylococcus aureus* and *Pseudomonas aeruginosa* dual-species biofilms grown in chronic wound-based models

Authors: Bikash Bhattarai[1] and Gordon F. Christopher[1*]

[1]Department of Mechanical Engineering, Whitacre College of Engineering, Texas Tech University, Lubbock TX
*Corresponding author: Gordon.Christopher@ttu.edu

Abstract

Wound infections become chronic due to biofilm formation by pathogenic bacteria; two such pathogens are *Staphylococcus aureus* and *Pseudomonas aeruginosa*. These bacteria are known to form polymicrobial biofilms in wounds, which exhibit increased colonization rates, enhanced chronicity, and greater resistance to treatment. Previously, the impacts of the wound bed environment on the mechanical properties of *P. aeruginosa* biofilms have been explored, and in this work the role of the wound bed environment on the viscoelasticity and microstructure of polymicrobial biofilms is characterized.

We hypothesize that common wound bed proteins mediate interactions between *S. aureus* and *P. aeruginosa* to enable the formation of more elastic and stiff biofilms. Growth media with varying protein content as well as additional collagen, a protein associated with wound extracellular matrix, were utilized to test our hypothesis.

Microrheology indicates that both *P. aeruginosa* and *S. aureus* form relatively stiffer single-species biofilms in wound environment with collagen. *S. aureus* produced stiffer biofilms in the presence of collagen, regardless of other wound proteins, likely due to its interactions with collagen. When both species were grown together in wound-like media, synergistic effects led to stiffer dual-species biofilms compared to their single-species forms. In all growth conditions, collagen significantly contributed to stiffening *P. aeruginosa/S. aureus* dual-species biofilms, suggesting it mediates complex interspecies interactions. High-resolution imaging and analysis revealed that collagen also influenced the microstructures of *P. aeruginosa/S. aureus* dual-species biofilms. In media containing wound proteins and collagen, *S. aureus* clusters were larger and exhibited more complex shapes. These results indicate that the wound bed environment not only provides improved antibacterial resistance due to cooperative interactions, but also improved mechanical protection, which impact common treatment methods like debridement.

INTRODUCTION

Biofilms are complicated structures composed of sessile bacterial cells encased into hydrogel of Extracellular Polymeric Substances (EPS), which consists of polysaccharides, proteins, nucleic acids and lipids creating a cohesive three-dimensional polymer network.[1, 2] Biofilms often are multispecies communities with bacteria species exhibiting complex interactions that influence the biofilm development[3, 4] and microstructure (clusters of single species microcolonies, clusters of co-aggregated species , or layered arrangement of individual species).[5] The interactions among bacteria species are influenced by the bacteria themselves through diffusing molecules[6, 7] and the surrounding environment,[8] and can be cooperative, competitive, or neutral in nature.[6-8]

Polymicrobial biofilms are particularly prevalent in medical infections.[9, 10] Studies indicate that collaborative interactions within wound based biofilms contribute to infection persistence by enhancing antibiotic resistance.[9] In humans, polymicrobial biofilm are frequently detected in oral infections, chronic wounds, respiratory infections such as cystic fibrosis, and in ear infections.[10] In chronic wound infections, 2 species are often found to coexist and form polymicrobial biofilms: *Pseudomonas aeruginosa* and *Staphylococcus aureus*.[10] *S. aureus*, in particular, is a major cause of nosocomial and community-acquired infections.[11] In chronic wounds *S. aureus* is often found close to the surface, whereas *P. aeruginosa* is observed to reside deeper in the wound bed.[12]

Due to their significance in medical infections,[10] biofilms formed by *P. aeruginosa* and *S. aureus,* and their inherent interactions are widely studied. An early study by DeLeon et. al., shows the synergistic effects on antibiotic tolerance of *in-vitro* biofilms grown from these two species.[13] Subsequent studies demonstrate how these two species support each other in colonizing the host and defying lethal antibiotics aiding infection chronicity.[14-19] Furthermore, non-motile *S. aureus* hitchhike with *P. aeruginosa* to relocate within an ecosystem [20, 21] through interactions between *S. aureus'* wall teichoic acids with *P. aeruginosa*'*s* lipopolysaccharides.[21]

Therapeutic approaches to remove *P. aeruginosa*/*S. aureus* biofilms from chronic wounds use a combination of physical removal via debridement followed by local treatment with high doses of antibiotics. Debridement of biofilms is crucial because biofilm matrix polysaccharides encase and protect the bacteria providing a diffusion barrier to antibiotics,[1, 2] and physical removal aids antibiotics in gaining deeper access to bacterial colonies within the wounds.[22, 23]

Debridement techniques include surgical, biological use of maggots, wet-to-dry dressings, irrigation, ultrasonic therapy, and/or enzymatic therapy to weaken biomass.[24, 25] Typically, multiple techniques are required for total removal.[25] The relationship between technique efficacy and biofilm viscoelasticity is not universal, since each method varies the application of stress/strain. It is unsurprising that different techniques have shown varying efficacy against biofilms from different species, which have different mechanical properties.[26, 27] Furthermore, heterogeneity in biofilm mechanical properties impacts local removal efficacy.[28] Specific debridement technique efficacy is influenced by the specific viscoelasticity of the treated biofilm.

Therefore, it is important to understand biofilm viscoelastic properties magnitude and heterogeneity to accurately select the appropriate method of debridement or to allow creation of biofilm models that will aid in debridement training.[29] Despite multiple studies looking at

polymicrobial interactions outlined above, the viscoelasticity of polymicrobial biofilms, particularly of *P. aeruginosa* and *S. aureus,* is not well characterized.

This problem is made difficult in part because although the coexistence of *P. aeruginosa* and *S. aureus* are evident *in-vivo*, competitive interactions resulting in the eradication of *S. aureus* are frequently observed *in-vitro* in common laboratory media.[13, 30-33] This is typically caused by several *P. aeruginosa* exoproducts.[32, 34-36] There are ways to create *in-vitro* models that mimic *in-vivo* synergistic activities. The inclusion of glucose, *S. aureus* preferred carbon source,[37, 38] in growth media has been found to aid co-culture. Including wound bed proteins in growth media has also been found to aid co-culture. Albumin in growth media inhibits *P. aeruginosa*'s ability to eliminate *S. aureus* by binding/sequestrating *P. aeruginosa*'s quorum-sensing molecules.[30] The Lubbock chronic wound biofilm model (WLM) successfully allows coculture[13] by mimicking the wound environment through inclusion of plasma and additional proteins.[39]

As reflected above, wound bed proteins play vital roles in influencing the interactions among *P. aeruginosa* and *S. aureus* species both *in-vitro* and *in-vivo*. However, it is unclear if these wound proteins impact polymicrobial biofilms viscoelasticity, which would impact effective debridement. The structure and mechanics of the biofilms are known to be strongly dependent on their growth environments.[40] Previous studies have shown that when collagen, a dominant protein found in wound bed extracellular matrix (ECM) which regulates wound healing,[41] is included in WLM media stiffer *P. aeruginosa* biofilms grow.[42, 43] However, it is not known how wound bed proteins in growth media impact viscoelasticity of polymicrobial biofilms.

This study's goal is to build upon previous findings of coexistence between bacteria in *in-vitro* wound-like environments to understand if interactions between bacteria and wound bed proteins impact polymicrobial biofilm mechanical properties. Specifically, this study investigates whether creating more wound-like growth media through inclusion of albumin and collagen aids in the formation of and impacts mechanical strength and heterogeneity of polymicrobial biofilms of *P. aeruginosa* and *S. aureus*. This is done through examination of microstructure, species dominance, and viscoelastic moduli on dual species biofilms using microrheology and high-resolution microscopy.

MATERIALS & METHODS

Bacteria growth medium preparation

Three growth medium conditions were chosen for the study: Luria-Bertani (LB) broth, LB broth with added Bovine Serum (LB/BS), and the Lubbock chronic wound biofilm model, also known as wound like media (WLM). LB (Luria-Bertani powder, Fisher Scientific, Catalog# BP1426-2) liquid broth solution was prepared by magnet-stirring LB powder in distilled water (5 grams of powder in 200 mL water). This fresh LB broth solution was then autoclaved for sterilization. Wound like media (WLM) was prepared by mixing 50%(v/v) Bovine Plasma (Fisher, Cat# 50-643-121), 45%(v/v) Bolton Broth (Fisher, Cat# OXCM0983B), and 5%(v/v) freeze thaw laked horse blood (VWR Cat# 10052-640) [39].

All experiments were repeated incorporating collagen in the growth medium. Collagen solution (2.352 mg/ml) was prepared by mixing collagen-I (Collagen-I, Rat, Corning 354236), 10x Phosphate Buffer Saline (Fisher Cat# BP3991), distilled water, and 1M NaOH as per manufacturer's instructions. Exact quantities of each element in solution depended on the concentration of collagen in solutions from manufacturer, which varied batch to batch.

Probe particle preparation

Carboxylate-modified negatively charged polystyrene microspheres (1 μm, Invitrogen, by ThermoFisherScientific, Cat# 13083) with red fluorescence (580nm/605nm) were used as probe particles. Red fluorescence allowed the particles to be distinguished from green fluorescence protein (GFP) expressing bacteria. The size and surface coatings of the particles were chosen such that they embed into the developing biofilm structure without passing through its pores/channels. [44] To clean particles prior to use, a series of three centrifugation steps were performed, at 6000 RPM for 10 minutes each. After each cycle, the supernatant was removed, and the particles were resuspended in fresh deionized water. After cleaning, a final particle solution was prepared having a concentration of $3x10^9$ particles/mL in an Eppendorf tube.

Bacterial strains and Biofilms growth

Table-1 provides the list of bacterial strains used for the study.[45-48] *P. aeruginosa* PAO1 and *S. aureus* SA31 wildtype strains were used to grow biofilms for microrheology, colony forming unit quantifications and Scanning Electron Microscopy (SEM). Fluorescent strains, PAO1 dsRed and SA RN4220, were used to grow biofilms for Confocal Laser Scanning Microscopy (CLSM). Frozen bacterial stocks were stored at -20°C. Prior to culturing, 10 mL of freshly prepared sterile LB liquid broth was added to a 100 mL Erlenmeyer flask. Using an inoculating loop, a small amount of frozen bacterial stock was added to the flask. Afterwards, the capped flask was incubated using a rotary shaker (Southwest Mini IncuShaker SH1000) at 200 rpm and 37°C for 24 hours. $10\mu L$ (approx. 10^7 CFU of bacterial cells) of the overnight culture of *P. aeruginosa*, *S. aureus*, or both ($5\mu L$ from each for the case of mixed species biofilms) was mixed with growth medium to prepare the inoculum for biofilm growth.

Strain	Type
P. aeruginosa PAO1	Wildtype
P. aeruginosa PAO1 dsRed	Genetically modified: Expresses red fluorescent protein (rfp)
S. aureus SA31	Wildtype
S. aureus RN4220	Genetically modified: Expresses green fluorescent protein (gfp)

Table 1: Bacterial strains used in the study.

Bacteria were inoculated into the microchannels using pipet tips filled with an inoculation solution of growth media and overnight culture as described below. All microchannels used in experiments were identical and fabricated out of polydimethylsiloxane (PDMS) using soft lithography as previously described.[49]

The LB inoculum included mixture of $10\mu L$ of overnight bacteria culture with $990\mu L$ of fresh LB broth. Particles sediment in the LB inoculum, adhering to slides and failing to incorporate into the

growing biofilm. Therefore, a particle solution with glycerol (to avoid sedimentation) was injected after 5 hours, ensuring particle incorporation in the biofilm matrix. This solution was made by mixing 1 mL of glycerol with 9 mL of freshly prepared LB broth. 3.5µL of the particle solution was vortex mixed with 1000µL of glycerol/LB solution, resulting in a solution with an estimated particle concentration of 10^7 particles/mL to create the injectable particle solution. This solution was then syringe pumped (@30 $\mu L/hr$ for 10 minutes) into the microchannels at 5 hours of inoculation.

For LB/BS growth medium, less particle sedimentation was observed due to the increased viscosity of LB/BS solution. Therefore, the particle incorporation into the broth did not require injection of particles after 5 hours or significant change to the growth medium. The LB/BS inoculum was prepared by mixing 3.5μL particle solution, 10μL of overnight bacteria culture, 100 μL Bovine Serum, 790μL of fresh LB broth, and 100 μL of glycerol (to ensure no sedimentation).

No significant sedimentation of particles was observed with WLM. The inoculum was prepared by mixing 3.5μL final particle solution, 10μL of overnight bacteria culture, and 990μL of WLM.

When repeating the experiments with collagen, 100μL of collagen solution previously prepared was accommodated in the inoculum of each case. This was achieved by reducing the equivalent volume (100μL) of fresh LB or WLM. 100µL collagen solution in the inoculum corresponds to 10% of its volume and contains collagen at a concentration of 0.2352 mg/mL.

After inoculation into the microchannels, the inlets and outlets were sealed with parafilm to prevent evaporation. The inoculated channels were kept inside an incubator at 37°C in static conditions to allow for biofilm growth. After 24 hours of inoculation, the biofilms were characterized via microrheology.

Passive Particle Tracking Microrheology

Particle tracking microrheology involves tracking the Brownian motion of particles embedded in a viscoelastic specimen. This technique probes microscale mechanical response with high spatiotemporal resolution without affecting specimen microstructure, and is thus well-suited for studying mechanics of heterogeneous materials like biofilms.[50-52] The probe particles trajectories are recorded and then the ensembled-averaged mean-squared-displacement (MSD), $\langle r^2(t)\rangle$, of individual particles as the function of their lag times, *t*, is calculated. The logarithmic slope of the MSD vs lag time, $\alpha = \frac{d(ln\langle r^2(t)\rangle}{d(\ln(t))}$, ranges from 0 to 1 and represents the relative viscoelasticity of the specimen: $\alpha = 1$ is purely viscous diffusion, $\alpha = 0$ is elastic, and values in between represent relative viscous/elastic nature of the material.[53] The creep compliance, or inverse stiffness, can also be calculated from MSD,

$$J(t) = \frac{3\pi a}{2k_BT}\langle r^2(t)\rangle \quad (1)$$

where, a = particle radius, k_B = Boltzmann Constant, and T= Temperature [54].

Epifluorescent microscopy (Nikon Eclipse Ti-E microscope, 50x magnification) with a single frequency excitation source (Spectra X light engine) was used to visualize fluorescent particles.

Particle movement was recorded as tiff stacks (Pco.edge 4.2 LT sCMOS) at 40 frames per second for 25 seconds. TrackMate plugin in the Fiji installation of ImageJ was then utilized to generate the particle tracks [55, 56]. Subpixel resolution of particle centroid locations was found using Laplacian of Gaussian filter and particle tracks were created with simple linear assignment. MATLAB was then used to calculate MSD, α, and J from particle trajectories using @msdanalyzer. [57] For each particle track, α was calculated for lowest 4% of lag times to ensure statistical significance.[58]

Use of video microscopy to track particles creates two primary errors: static and dynamic. Static errors are inherent measurement uncertainty caused by fluctuations in light intensity, vibrations, and camera resolution. Static error was determined by fixing probe particles in a strong gel (polydimethylsiloxane crosslinked at 10:1) and computing MSD, [59] providing a minimum static error threshold of ~0.003 μm^2 for the experimental setup used in this study. Dynamic errors occur from particle movement during exposure.[59-61] Evaluating dynamic errors is difficult in heterogeneous media. They were minimized keeping exposure times to 10% of the frame rate in all experiments.[60, 62]

Microrheology replicates

Biofilms were grown in four separate microchannels on a single chip. Within each microchannel, microrheology data was recorded from two distinct locations where separate biofilms were observed, resulting in four biological replicates with two technical replicates for each experiment. Although the same number of particles were mixed in all inoculums, the number of particles embedded within the biofilm matrix was stochastic. This resulted in varying numbers of particle tracks recorded for each experiment (Table 2).

	LB	LB and Collagen	LB/BS	LB/BS and Collagen	WLM	WLM and Collagen
P. aeruginosa	223	197	206	168	160	252
S. aureus	387	265	211	308	255	98
Dual species	237	142	266	247	185	127

Table 2: Number of particles tracked in each combination of strain and the growth medium.

Microrheological Data Analysis

Box-whisker plots were generated to represent the distributions of α and J from individual particle MSDs. The box is a representation of the middle 50% of the data, with the 'median' marked by a line inside the box and the 'mean' indicated by a black dot.

Unpaired Mann-Whitney test was conducted to observe the statistical differences in the median ranks of the rheological parameters of biofilms grown under different growth conditions. The Mann-Whitney test compares two independent groups to determine whether one group tends to have larger values than the other.

Qualitative interpretation of heterogeneity of data distributions can be identified by interpreting the relative size/range of boxes and whiskers from box-whisker plots. To provide a more

quantitative approach, the variances of data distributions were also calculated. Variance measures the degree of dispersion or variability in the data distributions. So, the distributions with larger variances tend to have more heterogeneous rheological properties compared to the distributions with lower variances. The Flinger-Killen test was implemented to find statistical differences in these variances. Thus, the variance values from these tables along with the Fligner-Kileen test will provide us with a clear understanding of data distributions with statistically higher or lower variances.

Both the Mann-Whitney test and Fligner-Kileen test are known for their robustness to non-parametric data.[63, 64] Statistical significance is demarcated in figures by * for $P \leq 0.05$, ** for $P \leq 0.01$, *** for $P \leq 0.001$ and **** for $P \leq 0.0001$. In all plots, statistical significances above the connecting lines compare the medians whereas the significances below the lines compare the variances between the data distributions.

Colony Forming Units (CFU) quantification and their statistical comparisons

Biofilms were grown in microchannels, pipetted out, and vortex mixed with 1x PBS. The biofilm mixed PBS solutions were subjected to serial dilutions and plated on isolation agars. The plated agars were incubated at 37°C overnight to allow colony formation, which were counted the following morning. CFU counts from four biological replicates were obtained for each experiment.

Statistical comparisons between the mean CFU values of bacterial cells within the biofilms grown under varying growth conditions were performed using the Tukey-Kramer Honest Significant Difference test.

Confocal and Electron Microscopy of the Biofilms

In-situ Confocal Laser Scanning Microscopy (CLSM) images of microchannel grown *P. aeruginosa/S. aureus* dual-species biofilms were obtained using Olympus FV3000 Scanning Confocal Microscope with 60x oil immersion objective. For each growth conditions, four CLSM images from four biological replicates were recorded for analysis.

Scanning Electron Microscopy (SEM) images were captured using a Zeiss crossbeam 540 scanning electron microscope. To prepare dual-species biofilms in PDMS microchannels for SEM, the procedure began by removing bottom glass slide from channels to expose biofilms, which were then washed with 0.1 M sodium cacodylate (Electron Microscopy Sciences) for 10 minutes and fixated using an enhanced primary technique developed by Wells and coworkers.[65] This method uses alcian blue (0.15% alcian blue), a cationic dye, as the primary fixative in addition to standard aldehydes (2% glutaraldehyde and 2% paraformaldehyde in 0.1M Sodium Cacodylate Buffer). The cationic dye forms ionic bonds with anionic components within the biofilm matrix enhancing the retention of extracellular polymeric substances. Biofilms were left to fix overnight, followed by three washes with 0.1 M sodium cacodylate each lasting 10 minutes. The buffer was then removed, and samples were stained with postfixative solution containing 1% osmium tetroxide (Ted Pella) and 1% tannic acid (Electron Microscopy Sciences). After 3 hours, the samples were washed with distilled water and dehydrated with graded alcohols for 15 minutes per step, starting with 10 minutes in 1:1 absolute ethanol (Thermo) to hexamethyldisilazane (HMDS, Ted Pella), followed by 100% HMDS for 5 minutes. The samples were air-dried for 30 minutes and mounted

onto clean SEM stubs using double-sided conductive tape (Ted Pella) and coated with a 12 nm layer of platinum/palladium using a Cressington 208HR sputter coater (Ted Pella).

Obtaining and analyzing the geometrical information of S. aureus clusters from Confocal Images

S. aureus clusters in the confocal images were identified as the continuous regions of green fluorescence. To obtain *S. aureus* cluster geometries, at first the CLSM images were thresholded to obtain binary images. Noises in the form of minute cluster-like geometries were then filtered by using a threshold area of 100 sq. pixels, which is less than 0.003% of the image area (Figure 1). This noise filtration was performed using the MATLAB 'bwareaopen' function which is a built-in MATLAB function used for removing small objects from binary images.

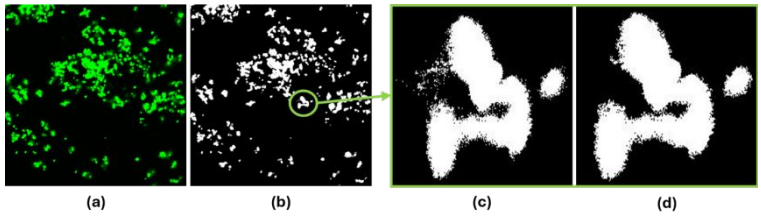

Figure 1: Thresholding and filtering background noise to obtain geometrical information from *S. aureus* clusters. (a) CLSM image of *S. aureus* fluorescent clusters obtained from dual-species biofilm imaging, (b) Image thresholded to obtain the binary image with *S. aureus* clusters, (c) An excerpt from the thresholded image showing *S. aureus* clusters with associated noise, (d) *S. aureus* clusters after noise filtration.

After filtering the noises, MATLAB 'regionprops' function was employed to obtain areas and perimeters of *S. aureus* clusters. The 'regionprops' is a powerful in-built MATLAB function that is used to measure properties of labeled image regions. It is widely applied in image processing and computer vision to extract shape, size and positional properties of objects in an image. It counts the number of pixels to determine the area, finds the average pixel position for the centroid, traces object boundaries for the perimeter, and fits basic geometry shapes (like rectangles or ellipses) to estimate properties like orientation and eccentricity.

Three metrics were used to analyze *S. aureus* cluster shapes: centroid to centroid distance, area, and the shape complexity, *S,*

$$S = \frac{P^2}{4\pi A} \quad (2)$$

p and A are perimeter and area of the cluster respectively: S is 1 if a cluster is a perfect circle and increasingly larger for more complex shapes.

Box whisker distributions of different parameters defined to examine *S. aurues* clusters were generated and statistical comparisons were performed. Again, the Mann-Whitney test and Fligner-Kileen tests were applied to test the differences between median ranks and the variances of the data distributions. Variance values of the geometrical parameters of *S. aureus* clusters are provided in Table 5.

RESULTS

Role of growth medium and collagen content on single species biofilms

Microrheological characterization of single-species *P. aeruginosa* and *S. aureus* biofilms were performed before investigating the dual-species biofilms. As outlined previously, we have chosen three different growth medium conditions; *P. aeruginosa* and *S. aureus* demonstrate different interactions in these growth conditions. These species display competitive interactions in LB broth but are cooperative and support the coexistence of each other in LB/BS and WLM [13, 30, 39]. Furthermore, we have investigated the impacts of Collagen on all single-species and dual-species *P. aeruginosa* and *S. aureus* biofilms grown in the growth medium conditions considered.

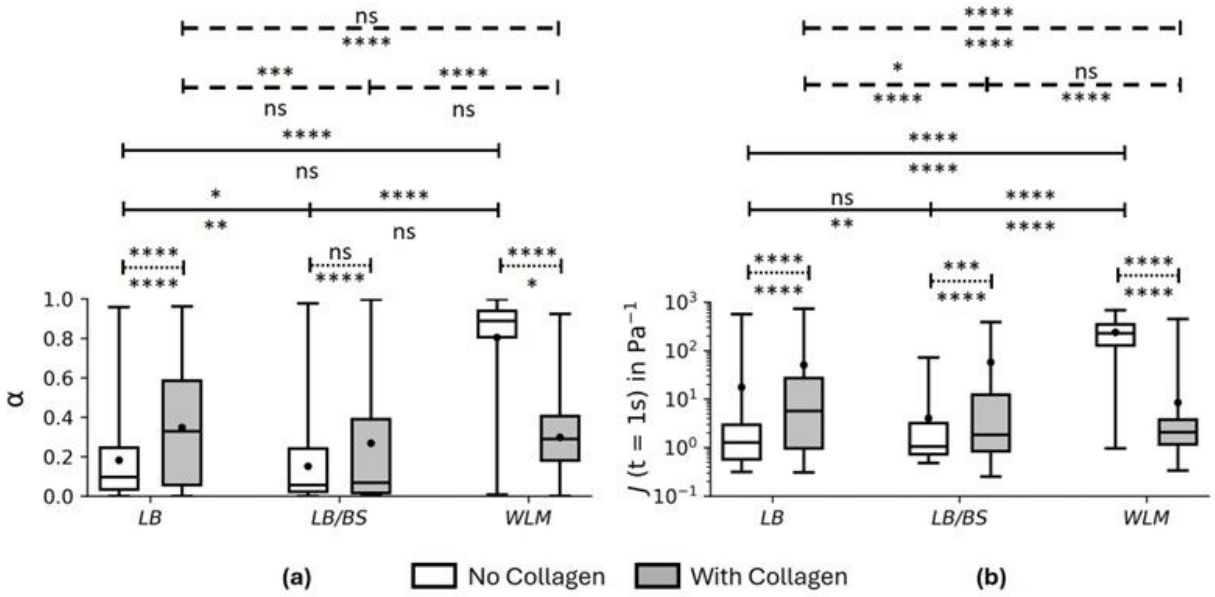

Figure 2: Relative viscoelasticity (a), creep compliance @1s (b), of *P. aeruginosa* single species biofilms grown under varying growth medium conditions for 24 hours. Statistical comparison between the same growth conditions with and without collagen are represented by dashed lines, between different growth conditions with no collagen are represented by a solid line, and between different growth conditions with collagen by a dashed line. Statistical significance is demarcated by * for P≤0.05, ** for P≤0.01, *** for P≤0.001 and **** for P≤0.0001. Significances above/below the connecting lines reflect the median/variance comparisons respectively.

As illustrated by Figure 1, *P. aeruginosa* formed relatively more elastic (lower α), and stiff (lower *J*) biofilms when grown in LB or LB/BS in comparison to WLM in absence of collagen. Across all growth conditions, there were no notable differences in CFUs of *P. aeruginosa* cells in the absence of collagen (Figure 2).

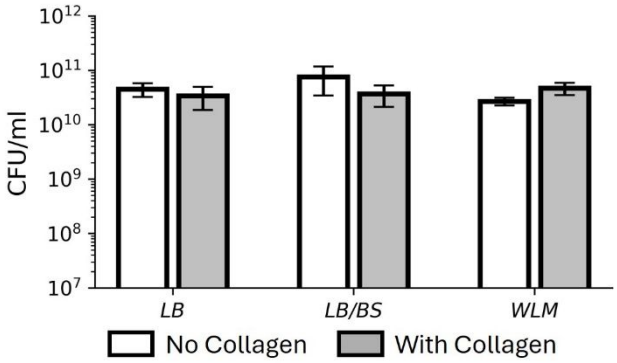

Figure 3: CFU quantifications of *P. aeruginosa* single species biofilms grown under varying growth medium conditions for 24 hours. Each bar represents the mean and its standard error, calculated from four biological replicates. Statistical comparisons were performed across all possible pairwise combinations of the six datasets, with no significant differences observed between any CFU pairs.

Following collagen incorporation into LB broth, *P. aeruginosa* biofilms exhibited significantly more viscous, compliant (Figure2) and heterogeneous properties based on increases in variances of these properties (Table 3 & 4). A similar trend of more viscous, compliant, and heterogeneous properties was observed in *P. aeruginosa* biofilms grown in LB/BS and collagen. However, after collagen incorporation in WLM *P. aeruginosa* biofilms were significantly stiffer, more homogeneous properties, and less compliant (Figure 2, Tables 3 and 4); this is consistent with previously observed effects for WLM grown biofilms and fundamentally different than the trends for LB and LB/BS.[42, 43] Similar to results without collagen, across all growth conditions, there was no notable difference in the CFU counts of bacterial cells within the biofilms (Figure 3).

	LB	LB and Collagen	LB/BS	LB/BS and Collagen	WLM	WLM and Collagen
P. aeruginosa	0.044	0.081	0.039	0.127	0.051	0.027
S. aureus	0.043	0.044	0.108	0.077	0.115	0.067
Dual species	0.046	0.037	0.132	0.091	0.138	0.018

Table 3: Variances of the $'\alpha'$ distributions of biofilms grown under varying growth conditions for 24 hours.

	LB	LB and Collagen	LB/BS	LB/BS and Collagen	WLM	WLM and Collagen
P. aeruginosa	4347	12417	76.99	13614	23735	1289
S. aureus	873	97	22018	203	14025	5682
Dual species	1384	1776	19591	4177	21054	3.0

Table 4: Variances of the $'J'$ distributions (in $1/Pa^2$) of biofilms grown under varying growth conditions for 24 hours.

In the absence of collagen, *S. aureus* grown in LB/BS biofilms had more heterogenous properties, more relatively elastic, but slightly more compliant (based on mean values) compared to those grown in LB (Figure 4, Tables 3 and 4). *S. aureus* biofilms grown in WLM compared to those in

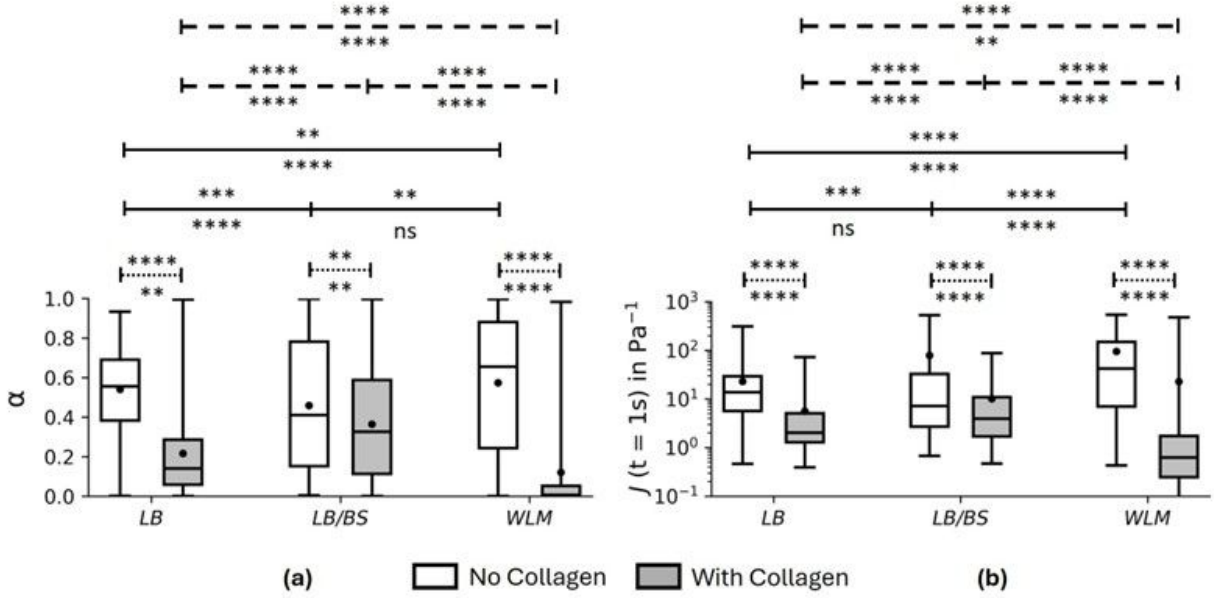

Figure 4: Relative viscoelasticity (a), creep compliance @1s (b), of *S. aureus* single species biofilms grown under varying growth medium conditions for 24 hours. Statistical comparison between the same growth conditions with and without collagen are represented by dashed lines, between different growth conditions with no collagen are represented by a solid lines, and between different growth conditions with collagen by a dashed line. Statistical significance is demarcated by * for P≤0.05, ** for P≤0.01, *** for P≤0.001 and **** for P≤0.0001. Significances above/below the connecting lines reflect the median/variance comparisons respectively.

LB or LB/BS without collagen were more compliant, and relatively viscous (Figure 4). These WLM grown *S. aureus* biofilms had relatively more heterogenous properties in comparison to LB grown biofilms (Figure 4, Tables 3 and 4). Across all growth media, no significant differences in the CFUs of *S. aureus* cells were observed in the absence of collagen (Figure 5).

With the addition of collagen, *S. aureus* biofilms became significantly stiffer, less compliant, and more homogeneous properties in LB/BS and WLM (Figure 4, Tables 3 and 4). In LB broth, *S. aureus* biofilms became significantly stiffer and less compliant after collagen incorporation. However, the effects on heterogeneity of properties were mixed, with α values exhibiting statistically greater variance after collagen addition, while J values showing less variance after collagen (Figure 4, Tables 3 and 4). There were some differences in CFUs of *S. aureus* cells between biofilms grown in LB and WLM before and after collagen addition with LB biofilms exhibiting less CFU and WLM exhibiting more (Figure 5).

Viscoelasticity and microstructure of dual-species P. aeruginosa/S. aureus biofilms

Dual-species *P. aeruginosa/S. aureus* biofilms grown in LB and in absence of collagen (Figure 6) behaved similarly to pure *P. aeruginosa* biofilms (Figure 2) with greater relatively elasticity and stiffness than pure *S. aureus* biofilms. In addition, results from the CFU quantifications of these LB broth grown dual-species biofilms show that *S. aureus* were roughly an order of magnitude less prevalent than *P. aeruginosa* after 24 hours (Figure 7). These results are consistent with Cendra and coworkers [37] who inoculated a similar CFU ratio into LB broth and found after 24 hours the CFUs of *S. aureus* were three orders of magnitude lower than those of *P. aeruginosa*. A potential explanation to the difference between studies is the disparity in growth

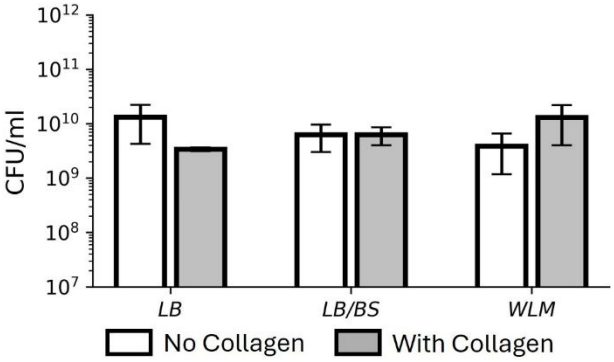

Figure 5: CFU quantifications of *S. aureus* single species biofilms grown under varying growth medium conditions for 24 hours. Each bar represents the mean and its standard error, calculated from four biological replicates. Statistical comparisons were performed across all possible pairwise combinations of the six datasets, with no significant differences observed between any CFU pairs.

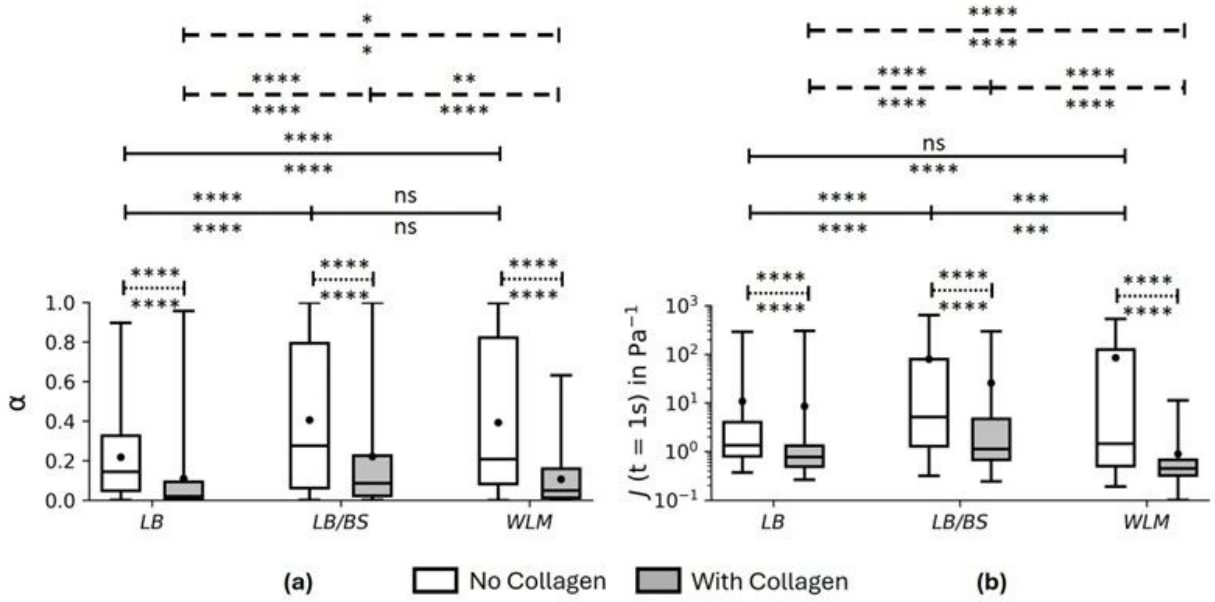

Figure 6: Relative viscoelasticity (a), creep compliance @1s (b), of dual species *P. aeruginosa/S. aureus* dual species biofilms grown under varying growth medium conditions for 24 hours. Statistical comparison between the same growth conditions with and without collagen are represented by dashed lines, between different growth conditions with no collagen are represented by a solid lines, and between different growth conditions with collagen by a dashed line. Statistical significance is demarcated by * for P≤0.05, ** for P≤0.01, *** for P≤0.001 and **** for P≤0.0001. Significances above/below the connecting lines reflect the median/variance comparisons respectively.

cells.

When grown in LB/BS without collagen, *P. aeruginosa/S. aureus* dual-species biofilms appeared to have a viscoelasticity (Figure 5) that is mix of viscoelastic characteristics of *P. aeruginosa* (Figure 1) and *S. aureus* (Figure 3) single species biofilms grown in LB/BS. This implies that with the addition of Bovine Serum in LB broth, both species co-existed and contributed to the dual-species biofilms' EPS. Their co-operative coexistence was also reflected in the CFU quantification results as the biofilms possessed a similar quantity of both *P. aeruginosa* and *S. aureus* cells (Figure 7).

In WLM without collagen, the viscoelastic properties of *P. aeruginosa/S. aureus* dual-species biofilms were comparable to those of LB/BS no-collagen biofilms (Figure 6). However, the dual-species biofilms exhibited greater elasticity and reduced compliance (Figure 5) compared to both single-species *P. aeruginosa* (Figure 1) or *S. aureus* (Figure 3) biofilms grown in WLM without collagen. Consistent with expectations in WLM, the CFU results also indicated comparable populations of *P. aeruginosa* and *S. aureus* within these dual-species biofilms (Figure 7).

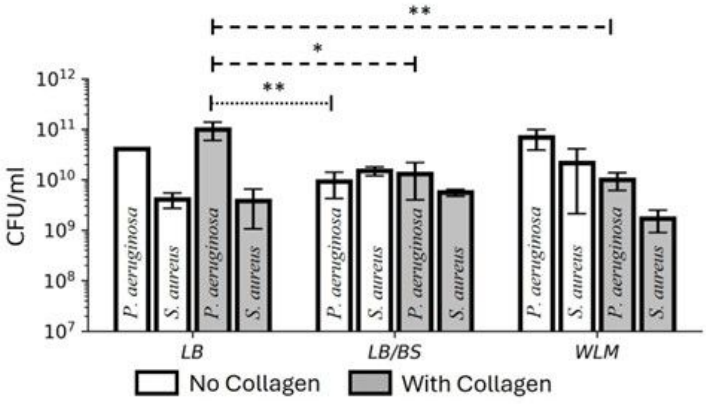

Figure 7: CFU quantifications of *P. aeruginosa/S. aureus* dual species biofilms grown under varying growth medium conditions for 24 hours. Each bar represents the mean and its standard error, calculated from four biological replicates. Statistical comparisons were conducted across all possible pairwise combinations of the twelve datasets, revealing some significant differences. Notably, *P. aeruginosa* populations in dual-species biofilms grown in LB with collagen were higher than those in dual-species biofilms grown under other conditions.

In all growth media, dual-species *P. aeruginosa/S. aureus* biofilms grown with collagen exhibited significantly higher elasticity, stiffness, and homogeneity of properties compared to those without collagen (Figure 6). Additionally, CFU quantifications for biofilms in LB and LB/BS with collagen were comparable to biofilms grown without collagen in these media (Figure 7). However, in WLM with collagen, the CFU results showed a slightly reduced *S. aureus* population relative to *P. aeruginosa* within the dual-species biofilms (Figure 7).

One potential way to evaluate how the collagen is impacting the interactions between the EPS components of the biofilms and/or bacteria is their spatial organization,[66-69] which could also help to understand the observed mechanical changes. High resolution images of *P. aeruginosa/S. aureus* polymicrobial biofilms grown under all growth conditions considered are therefore shown in Figures 8.

CLSM images of dual-species *P. aeruginosa/S. aureus* biofilms grown in LB broth regardless of collagen presence revealed small colonies of *S. aureus* cells (green fluorescent) amongst the

predominant *P. aeruginosa* cells (red fluorescent) (Figure 8). *S. aureus* formation into small-colonies to survive *P. aeruginosa*'s attack in laboratory growth media has been previously described.[32, 33] In SEM images, *P. aeruginosa* alone cells are seen embedded and dispersed throughout the EPS matrix in both with and without collagen biofilms. Qualitatively, there is no difference between the microstructure based on bacteria location in Figure 8 that would explain the differences between the with and without collagen biofilms as observed in Figure 6.

In LB/BS with/without Collagen, *P. aeruginosa/S. aureus* dual-species biofilms had clumps of green-fluorescent *S. aureus* cells among the dispersed *P. aeruginosa* cells (Figure 8). Furthermore, *P. aeruginosa* cells are also colocalized with the *S. aureus* cells in *S. aureus* clumps as revealed by higher magnification SEM images. The integrated microstructure is notably different than the LB alone and may explain the difference between it and the LB/BS without collagen. However, similar to LB medium there is qualitatively no difference between the microstructure based on bacteria location in Figure 8 that would explain the differences between the LB/BS with and without collagen biofilms as observed in Figure 6, or the commonality of behavior between the LB and LB/BS biofilms with collagen.

Finally, CLSM and SEM images of dual-species biofilms grown in WLM with/without Collagen revealed they have features similar to dual-species LB/BS grown biofilms with *S. aureus* clusters among *P. aeruginosa* cells (Figure 8). Again, the integrated structure may indicate differences between LB and WLM but does not aid in understanding differences between with/without collagen WLM and the commonality in the with collagen results.

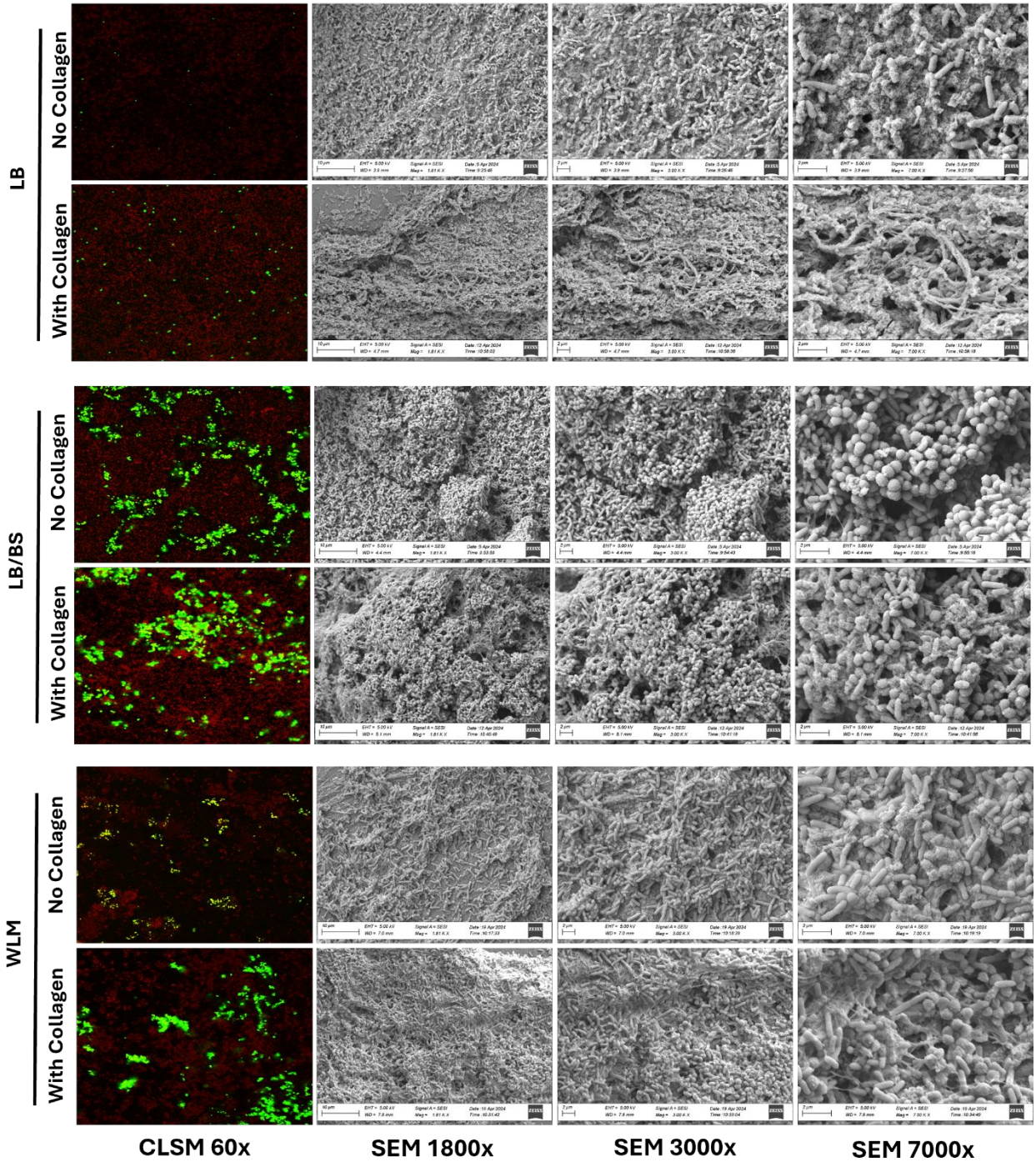

Figure 8: CLSM and SEM of *P. aeruginosa/S. aureus* dual-species biofilms grown in varying growth conditions for 24 hours. In CLSM images, *P. aeruginosa* are red fluorescent and the *S. aureus* are green fluorescent. Likewise, as reflected in SEM images, bacterial cells with cylindrical geometry are *P. aeruginosa* whereas the *S. aureus* cells have spherical geometry. For each growth condition, four CLSM images were captured from four biological replicates, and three SEM images were obtained from three biological replicates. A representative image from each case is shown in the figure above.

DISCUSSION

Impact of growth media and collagen content on single species biofilms

P. aeruginosa formed apparently viscous biofilms in WLM alone but formed significantly stiffer biofilms with WLM and collagen. This effect on the viscoelasticity of *P. aeruginosa* biofilms with collagen incorporation in WLM was also noted in a previous study.[42] WLM comprises components that closely mimic the host environment whereas the other two medium are primarily the LB broth, a common laboratory nutrient-rich medium.[39] This discrepancy in viscoelasticity results suggests that *P. aeruginosa*' s ability to form mechanically stronger biofilms in presence of collagen is dependent upon the host-like environment offered by the WLM. Interestingly, these results are supported by another prior study where *P. aeruginosa* formed further stiffer biofilms when grown in in-vivo wounds.[43]

Likewise, in all three growth medium cases, *S. aureus* showed a consistent behavior forming relatively more rigid biofilms in presence of collagen. Among several cell surface adhesion proteins produced by *S. aureus*, *Cna* is known to have collagen binding, bacterium-host adherence, and immune evasion properties.[70, 71] The *Cna*-collagen binding has been linked to worse patient outcomes in bone related [72, 73] and bloodstream infections [74]. The findings of this work indicate that *S. aureus* potentially shows another antagonistic effect in the presence of collagen by forming stiffer biofilms in wound environments.

The microrheological study of *P. aeruginosa* and *S. aureus* single-species biofilms demonstrated varying mechanical integrity and heterogeneity of properties when grown in different grown media indicating that the growth media play a crucial role in interactions among EPS components of each bacteria, which in turn impacts the mechanical properties. These mechanical differences are likely due to microstructural changes brough about by the growth medium such as changes to EPS polysaccharide conformation, entanglement of growth medium proteins with EPS polysaccharides, increase in specific EPS component expression, or changes to EPS crosslinking due to environmental conditions. Mechanical changes would appear to have little to do with increased bacterial growth rates, since similar CFUs of bacterial cells across all growth conditions for each species were observed. Additional studies are needed to fully understand the differences in composition and interactions among the biofilm matrix components under different growth conditions at the molecular level.

Impact of Growth media on dual species biofilms in the absence of Collagen

Dual-species *P. aeruginosa/S. aureus* biofilms grown in LB were relatively elastic (Figure 9) and closely resembled the viscoelastic characteristics of *P. aeruginosa* single species biofilms grown in LB. Previous findings indicate that *P. aeruginosa* readily eradicates the *S. aureus* in LB broth [13, 30], which is consistent with the observations of CFU count in Figure 6. *P. aeruginosa*'s attack on *S. aureus* likely accounts for its dominance over the viscoelastic properties of the dual species biofilms. It was suspected that *S. aureus* might contribute to the initial stages of biofilm formation when it has a more equal share of CFUs, which might impact overall biofilm development and physical properties. However, the results appear to reject this hypothesis, and lead to the possibility that *P. aeruginosa*'s exoproducts may also inhibit *S. aureus*'s ability to release any EPS. Although

several studies that have demonstrated the reduction of *S. aureus*'s CFUs in laboratory growth media due to *P. aeruginosa*, there are no studies, to our knowledge, investigating whether *S. aureus* contributes the initial EPS composition of a dual species biofilm grown in LB.

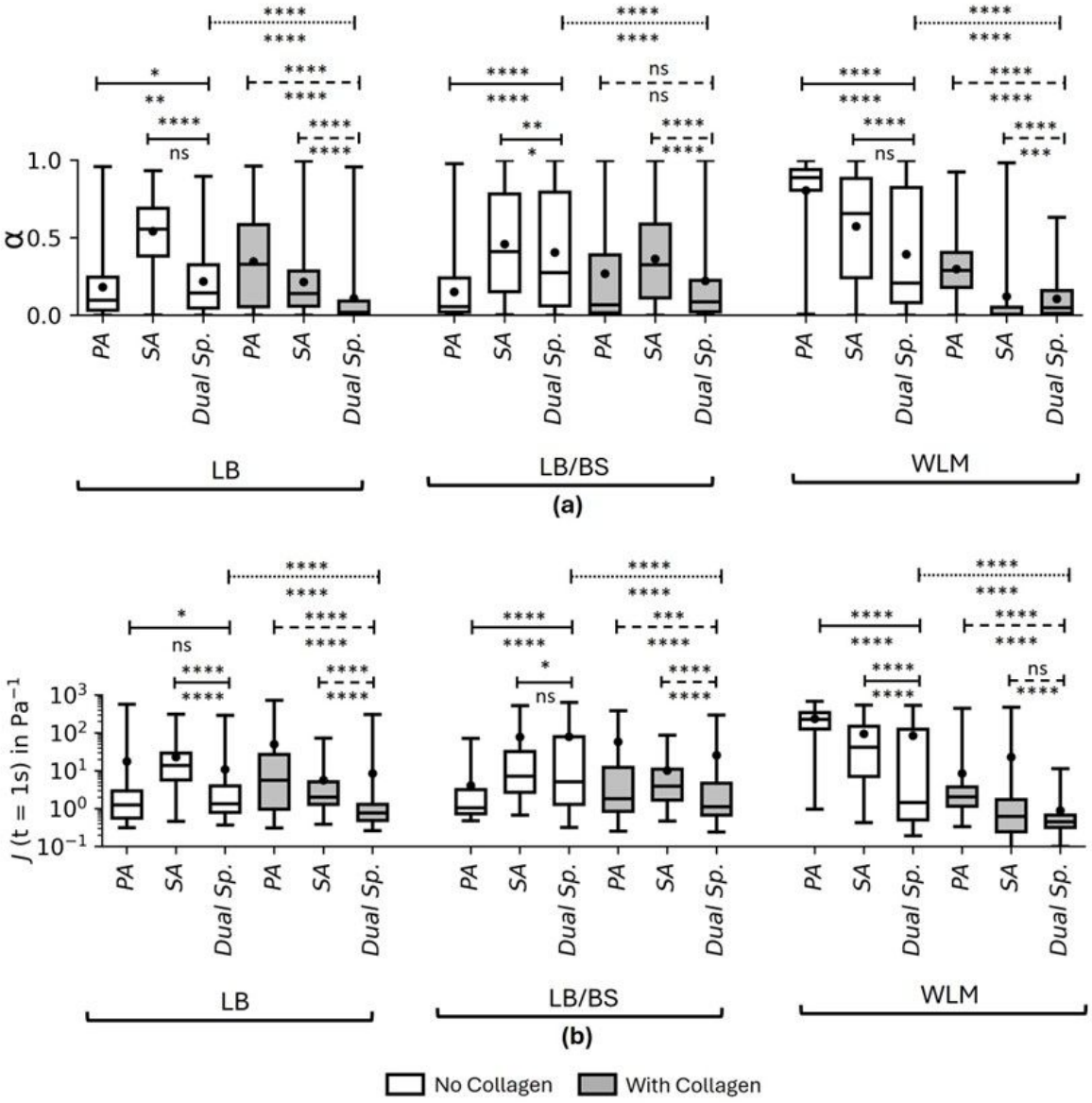

Figure 9: Relative viscoelasticity (a), creep compliance @1s (b), of single and dual species *P. aeruginosa/S. aureus* biofilms grown under varying growth medium conditions for 24 hours. Statistical comparison between the same growth conditions with and without collagen are represented by dashed lines, between different growth conditions with no collagen are represented by a solid lines, and between different growth conditions with collagen by a dashed line. Statistical significance is demarcated by * for P≤0.05, ** for P≤0.01, *** for P≤0.001 and **** for P≤0.0001. Significances above/below the connecting lines reflect the median/variance comparisons respectively.

In WLM and LB/BS (Figure 9), the viscoelastic behavior of *P. aeruginosa/S. aureus* dual-species biofilms were not so clearly dominated by one species and CFU counts were similar between the 2 species (Figure 6). In LB/BS, the co-cultured had more heterogeneous properties than the single species biofilms with stiffness and relative viscosity in between the single species behaviors (Table

3&4). Likewise, co-culture biofilms in WLM also appeared more heterogeneous in their properties (Table 3&4) but were more elastic and less compliant than WLM grown single species biofilms. Biofilms grown in WLM are previously described to display synergism to defy antibiotic treatments attributed to host derived or bacterium derived matrix components [13, 39]. Our observations indicate they also tend to form their mixed biofilm matrix more strongly in wound environments.

Impact of Collagen on dual species biofilms

P. aeruginosa/S. aureus dual-species biofilms became more stiffer, less compliant, and homogeneous in all growth conditions with collagen in comparison to those without collagen. Results from single-species *S. aureus* biofilms indicated interaction between *S. aureus* or its EPS components with collagen, making the biofilms stiffer and have more homogenous properties (Figure 3, Table 3, Table 4). So, for dual-species biofilms grown with collagen in LB/BS or WLM where *S. aureus* is abundant, there is assumption that *S. aureus*'s continues to interact with collagen to increase overall biofilms stiffness and elasticity. Additionally, in WLM, both species formed stiffer single-species biofilms with collagen, indicating more complex interactions may be occurring.

Dual-species biofilm's stiffness increased after collagen inclusion in LB-only media as well, where *S. aureus* population was negatively impacted by the *P. aeruginosa* (Figure 6), and hence it was expected the low stiffness/elasticity of the *P. aeruginosa* biofilm would still dominate as it did without collagen. Because of *S. aureus*'s interactions with collagen, collagen might have mediated a more cooperative set of interactions among these species, enabling the formation of biofilms with greater elasticity across all conditions, as hypothesized earlier.

A more quantitative approach is taken to further understand the effects of collagen in dual species biofilms by examining the *S. aureus*' structures specifically for changes in size and shape/complexity of *S. aureus* clusters. Geometries of *S. aureus* clusters were obtained as described previously in the methods section.

	LB	LB and Collagen	LB/BS	LB/BS and Collagen	WLM	WLM and Collagen
Distance	255262	266151	245362	254996	267263	263306
Area	35996	16585	3174280	10276803	500880	29183202
Shape complexity factor	1.62	0.39	5.60	6.92	2.09	14.98

Table 5: Variances of the geometrical parameters of *S. aureus* clusters observed in CLSM images of dual-species biofilms grown under varying growth conditions for 24 hours.

Statistically, there appeared to be some effects of collagen on both the medians and variances of the centroid distributions across all growth conditions (Figure 10). However, a general observation of the distributions reflects no significant changes in the spatial arrangement of the clusters. The statistically significant differences observed may be attributed to the large number of data points of distances, which were well over 10,000 for each system.

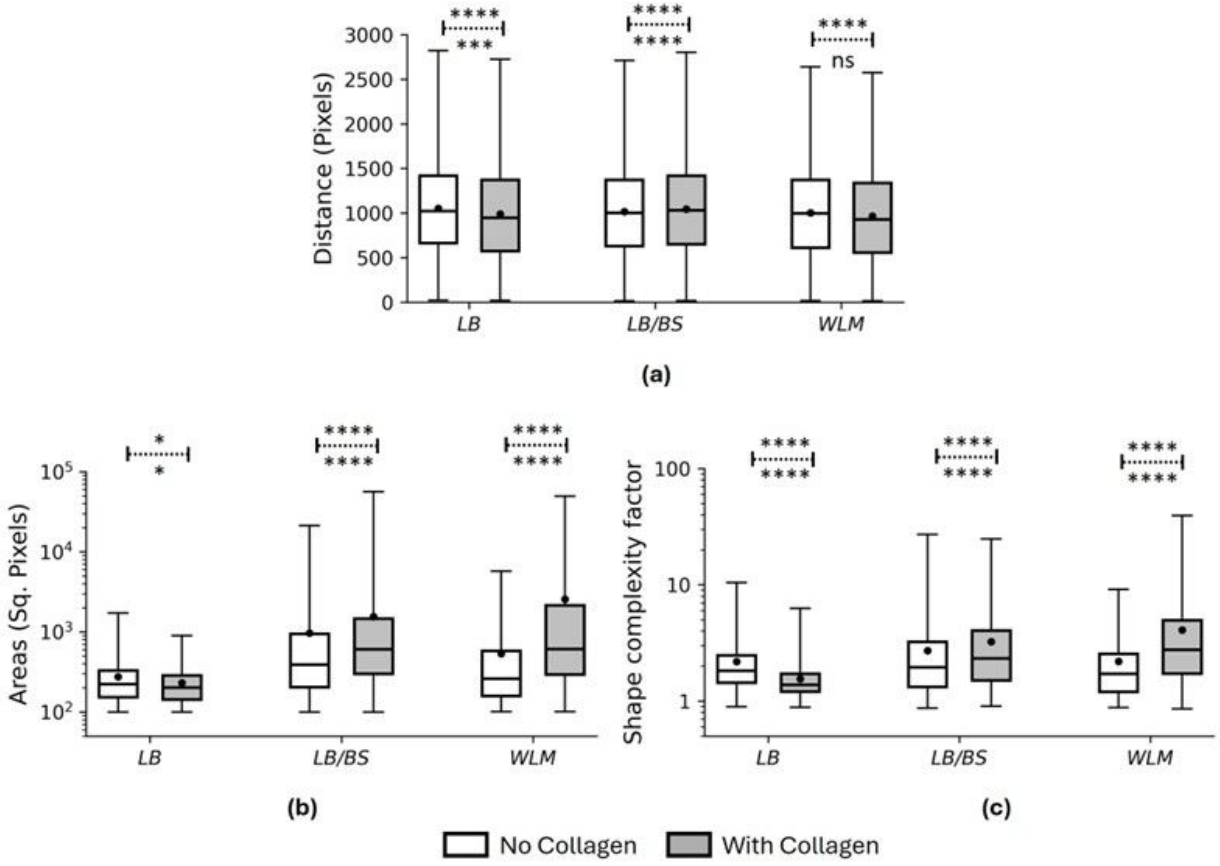

Figure 10: Distributions of (a) distances between the *S. aureus* cluster centroids, (b) areas of *S. aureus* clusters, and (c) shape complexity factors of *S. aureus* clusters, as observed in CLSM images of *P. aeruginosa/S. aureus* dual-species biofilms grown in varying growth conditions for 24 hr. Statistical comparison between the same growth conditions with and without collagen are represented by dashed lines, between different growth conditions with no collagen are represented by a solid lines, and between different growth conditions with collagen by a dashed line. Statistical significance is demarcated by * for P≤0.05, ** for P≤0.01, *** for P≤0.001 and **** for P≤0.0001. Significances above/below the connecting lines reflect the median/variance comparisons respectively.

In LB broth, the incorporation of collagen resulted in *S. aureus* microcolonies with reduced areas and less complex shapes, which may indicate sequestration of EPS/bacteria as previously hypothesized. For the WLM and LB/BS broth, results showed that in polymicrobial biofilms grown in LB/BS and WLM with collagen, *S. aureus* clusters had significantly larger areas and more complex shapes (Figure 10). In addition, after collagen incorporation, the areas and shape factors of *S. aureus* clusters showed reduced variance in LB broth but exhibited increased variability in LB/BS and WLM (Figure 10, Table 5). This suggests that the presence of collagen can lead to different effects on the microstructures of *S. aureus* depending on whether their interactions with *P. aeruginosa* are competitive (LB) or collaborative (LB/BS and WLM). In

conditions of cooperative interaction, the abundance of *S. aureus* and its interactions with collagen likely contributed to the formation of larger and more complex-shaped clusters. Therefore, it is possible to assume that the differences in behavior between the without collagen biofilms can be attributed to the differences observed in microstructure between the LB with the LB/BS and WLM. Furthermore, the increased stiffness of the LB/BS and WLM with addition of collagen could in part be due to the observed changes in Figure 10.

However, these factors alone cannot explain the universal impact of collagen to create more stiff, elastic, and homogenous properties in polymicrobial biofilms, given LB broth shows different microstructural behavior. Closer examination of the high magnification SEM images does provide some insight into this condition. In all dual species biofilms grown in media with collagen, fiber like structures are observed enmeshed into the biofilm that are not seen in the without collagen media results. It is reasonable to assume that these are in fact collagen fibers forming in the media, and then physically entangling into all biofilms as they grow, regardless of growth conditions. We may further conclude that the formation/enmeshing of these fibers is in part due to the presence of the *S. aureus*, since the single species *P. aeruginosa* do not universally exhibit this ability.

Conclusion

Chronic wounds often contain polymicrobial biofilms formed by *P. aeruginosa* and *S. aureus*. Due to their significance in chronic wound infections, this work most importantly explored the impacts of wound environments and collagen on their single-species and polymicrobial biofilms viscoelasticity. We observed significant changes in viscoelasticity across the various growth conditions, particularly when wound bed proteins were included, which will impact the efficacy of various debridement techniques.

In all media tested, both *P. aeruginosa* and *S. aureus* formed elastic single-species biofilms. However, their reaction to the inclusion of collagen was notably different. *S. aureus* formed stiffer biofilms in the presence of collagen, regardless of wound protein presence, likely due to its known interactions with collagen. In WLM, *P. Aeruginosa* biofilms were also stiffer in the presence of collagen, similar to previous studies.[42] Interestingly, collagen actually had a weakening effect in LB and LB/BS media, which was a departure from previous work, indicating that interactions between collagen and *P. aeruginosa* are mediated by proteins found in the wound that are also in WLM. Wound bed environment contains other host components such as fibrinogen, elastin, and immune cells;[75] further studies are required to investigate which of these mediates the interaction between collagen and *P. aeruginosa.*

Synergistic effects were observed when both species were grown together in WLM, resulting in stiffer dual-species biofilms compared to their single-species counterparts, which was not observed for the LB or LB/BS media. These results indicate that previously observed synergistic activities between these species in WLM[13] extend to creating stiffer biofilms, which has not previously been reported.

The incorporation of collagen further increased the stiffness of dual-species biofilms in all growth media, indicating it mediates complex interactions between the two species. This was confirmed via the high-resolution imaging that showed collagen impacts the microstructure of *S. aureus* clusters within polymicrobial biofilms. These clusters became larger and had more complex shapes

in growth media with wound proteins and collagen. However, the most likely cause of this increase appears to be the inclusion of the collagen fibrils observed in SEM images.

Acknowledgements

The authors gratefully acknowledge support from DOE/NNSA MSIPP Growing STEMS (grant number DOE NA0003988) and Dr. Betsy Snell, Program Manager. The authors would like to thank Dr. Kendra Rumbaugh and her student Hui Hua from TTUHSC for their help throughout the work.

REFERENCES

1. H. C. Flemming and J. Wingender, *Nature Reviews Microbiology*, 2010, **8**, 623-633.
2. B. W. Peterson, Y. He, Y. J. Ren, A. Zerdoum, M. R. Libera, P. K. Sharma, A. J. van Winkelhoff, D. Neut, P. Stoodley, H. C. van der Mei and H. J. Busscher, *Fems Microbiol Rev*, 2015, **39**, 234-245.
3. T. Ouidir, B. Gabriel and Y. Nait Chabane, *J Biotechnol*, 2022, **350**, 67-74.
4. A. Luo, F. Wang, D. Sun, X. Liu and B. Xin, *Front Microbiol*, 2021, **12**, 757327.
5. E. J. Stewart, D. E. Payne, T. M. Ma, J. S. VanEpps, B. R. Boles, J. G. Younger and M. J. Solomon, *Appl Environ Microbiol*, 2017, **83**.
6. V. Gordon, L. Bakhtiari and K. Kovach, *Phys Biol*, 2019, **16**, 041001.
7. Q. Li, L. Liu, A. L. Guo, X. S. Zhang, W. K. Liu and Y. Ruan, *J Food Protect*, 2021, **84**, 2071-2083.
8. P. Moons, C. W. Michiels and A. Aertsen, *Crit Rev Microbiol*, 2009, **35**, 157-168.
9. R. A. Gabrilska and K. P. Rumbaugh, *Future Microbiol*, 2015, **10**, 1997-2015.
10. V. T. Anju, S. Busi, M. Imchen, R. Kumavath, M. S. Mohan, S. A. Salim, P. Subhaswaraj and M. Dyavaiah, *Antibiotics-Basel*, 2022, **11**.
11. J. L. Lister and A. R. Horswill, *Front Cell Infect Microbiol*, 2014, **4**, 178.
12. M. Fazli, T. Bjarnsholt, K. Kirketerp-Moller, B. Jorgensen, A. S. Andersen, K. A. Krogfelt, M. Givskov and T. Tolker-Nielsen, *J Clin Microbiol*, 2009, **47**, 4084-4089.
13. S. DeLeon, A. Clinton, H. Fowler, J. Everett, A. R. Horswill and K. P. Rumbaugh, *Infection and Immunity*, 2014, **82**, 4718-4728.
14. T. Beaudoin, Y. C. W. Yau, P. J. Stapleton, Y. Gong, P. W. Wang, D. S. Guttman and V. Waters, *NPJ Biofilms Microbiomes*, 2017, **3**, 25.
15. G. Orazi and G. A. O'Toole, *mBio*, 2017, **8**.
16. L. Radlinski, S. E. Rowe, L. B. Kartchner, R. Maile, B. A. Cairns, N. P. Vitko, C. J. Gode, A. M. Lachiewicz, M. C. Wolfgang and B. P. Conlon, *PLoS Biol*, 2017, **15**, e2003981.
17. C. Cigana, I. Bianconi, R. Baldan, M. De Simone, C. Riva, B. Sipione, G. Rossi, D. M. Cirillo and A. Bragonzi, *J Infect Dis*, 2018, **217**, 933-942.
18. G. Millette, J. P. Langlois, E. Brouillette, E. H. Frost, A. M. Cantin and F. Malouin, *Front Microbiol*, 2019, **10**, 2880.
19. E. Y. Trizna, M. N. Yarullina, D. R. Baidamshina, A. V. Mironova, F. S. Akhatova, E. V. Rozhina, R. F. Fakhrullin, A. M. Khabibrakhmanova, A. R. Kurbangalieva, M. I. Bogachev and A. R. Kayumov, *Sci Rep*, 2020, **10**, 14849.
20. T. Samad, N. Billings, A. Birjiniuk, T. Crouzier, P. S. Doyle and K. Ribbeck, *ISME J*, 2017, **11**, 1933-1937.
21. C. C. Liu and M. H. Lin, *Front Microbiol*, 2022, **13**, 1068251.
22. D. Fleming and K. P. Rumbaugh, *Microorganisms*, 2017, **5**.
23. V. D. Gordon, M. Davis-Fields, K. Kovach and C. A. Rodesney, *J Phys D Appl Phys*, 2017, **50**.
24. S. K. McCallon, D. Weir and J. C. Lantis, 2nd, *J Am Coll Clin Wound Spec*, 2014, **6**, 14-23.
25. R. K. Thapa, J. O. Kim and J. Kim, *Journal of Pharmaceutical Investigation*, 2023, **53**, 627-641.
26. H. N. Wilkinson, A. J. McBain, C. Stephenson and M. J. Hardman, *Advances in wound care*, 2016, **5**, 475-485.
27. K. Ousey and L. Ovens, *Journal of Wound Care*, 2023, **32**, S4-S10.

28. B. W. Peterson, Y. He, Y. Ren, A. Zerdoum, M. R. Libera, P. K. Sharma, A.-J. Van Winkelhoff, D. Neut, P. Stoodley and H. C. Van Der Mei, *Fems Microbiol Rev*, 2015, **39**, 234-245.
29. J. J. Senior, K. Jaworska, L. Atkin, K. Ousey and A. M. Smith, *In vitro models*, 2024, 1-9.
30. A. C. Smith, A. Rice, B. Sutton, R. Gabrilska, A. K. Wessel, M. Whiteley and K. P. Rumbaugh, *Infect Immun*, 2017, **85**.
31. M. A. Alford, S. Mann, N. Akhoundsadegh and R. E. W. Hancock, *Sci Rep-Uk*, 2022, **12**.
32. L. R. Hoffman, E. Deziel, D. A. D'Argenio, F. Lepine, J. Emerson, S. McNamara, R. L. Gibson, B. W. Ramsey and S. I. Miller, *Proc Natl Acad Sci U S A*, 2006, **103**, 19890-19895.
33. L. Biswas, R. Biswas, M. Schlag, R. Bertram and F. Gotz, *Appl Environ Microbiol*, 2009, **75**, 6910-6912.
34. E. Kessler, M. Safrin, J. C. Olson and D. E. Ohman, *J Biol Chem*, 1993, **268**, 7503-7508.
35. Y. Liu, E. S. Gloag, P. J. Hill, M. R. Parsek and D. J. Wozniak, *J Bacteriol*, 2022, **204**, e0007622.
36. L. E. P. Dietrich, A. Price-Whelan, A. Petersen, M. Whiteley and D. K. Newman, *Mol Microbiol*, 2006, **61**, 1308-1321.
37. M. D. M. Cendra, N. Blanco-Cabra, L. Pedraz and E. Torrents, *Sci Rep*, 2019, **9**, 16284.
38. L. Kvich, S. Crone, M. H. Christensen, R. Lima, M. Alhede, M. Alhede, D. Staerk and T. Bjarnsholt, *J Bacteriol*, 2022, **204**, e0017422.
39. Y. Sun, S. E. Dowd, E. Smith, D. D. Rhoads and R. D. Wolcott, *Wound Repair Regen*, 2008, **16**, 805-813.
40. H. Boudarel, J. D. Mathias, B. Blaysat and M. Grédiac, *Npj Biofilms Microbi*, 2018, **4**.
41. S. S. Mathew-Steiner, S. Roy and C. K. Sen, *Bioengineering-Basel*, 2021, **8**.
42. M. U. Rahman, D. F. Fleming, I. Sinha, K. P. Rumbaugh, V. D. Gordon and G. F. Christopher, *Soft Matter*, 2021, **17**, 6225-6237.
43. M. U. Rahman, D. F. Fleming, L. Wang, K. P. Rumbaugh, V. D. Gordon and G. F. Christopher, *NPJ Biofilms Microbiomes*, 2022, **8**, 49.
44. S. C. Chew, B. Kundukad, T. Seviour, J. R. C. van der Maarel, L. Yang, S. A. Rice, P. Doyle and S. Kjelleberg, *Mbio*, 2014, **5**.
45. B. W. Holloway, V. Krishnapillai and A. F. Morgan, *Microbiol Rev*, 1979, **43**, 73-102.
46. C. M. Watters, T. Burton, D. K. Kirui and N. J. Millenbaugh, *Infect Drug Resist*, 2016, **9**, 71-78.
47. I. Frost, W. P. J. Smith, S. Mitri, A. San Millan, Y. Davit, J. M. Osborne, J. M. Pitt-Francis, R. C. MacLean and K. R. Foster, *Isme Journal*, 2018, **12**, 1582-1593.
48. C. L. Malone, B. R. Boles, K. J. Lauderdale, M. Thoendel, J. S. Kavanaugh and A. R. Horswill, *J Microbiol Meth*, 2009, **77**, 251-260.
49. B. Bhattarai and G. F. Christopher, *Front Phys-Lausanne*, 2023, **11**.
50. J. A. McGlynn, N. Wu and K. M. Schultz, *J Appl Phys*, 2020, **127**.
51. N. Billings, A. Birjiniuk, T. S. Samad, P. S. Doyle and K. Ribbeck, *Rep Prog Phys*, 2015, **78**, 036601.
52. A. Birjiniuk, N. Billings, E. Nance, J. Hanes, K. Ribbeck and P. S. Doyle, *New J Phys*, 2014, **16**, 085014.
53. T. Savin and P. S. Doyle, *Physical Review E*, 2007, **76**, 021501.
54. T. A. Waigh, *Reports on Progress in Physics*, 2005, **68**, 685-742.
55. J. Y. Tinevez, N. Perry, J. Schindelin, G. M. Hoopes, G. D. Reynolds, E. Laplantine, S. Y. Bednarek, S. L. Shorte and K. W. Eliceiri, *Methods*, 2017, **115**, 80-90.

56. J. Schindelin, I. Arganda-Carreras, E. Frise, V. Kaynig, M. Longair, T. Pietzsch, S. Preibisch, C. Rueden, S. Saalfeld, B. Schmid, J.-Y. Tinevez, D. J. White, V. Hartenstein, K. Eliceiri, P. Tomancak and A. Cardona, *Nature Methods*, 2012, **9**, 676-682.
57. N. Tarantino, J.-Y. Tinevez, E. F. Crowell, B. Boisson, R. Henriques, M. Mhlanga, F. Agou, A. Israël and E. Laplantine, *Journal of Cell Biology*, 2014, **204**, 231-245.
58. X. Michalet, *Phys Rev E Stat Nonlin Soft Matter Phys*, 2010, **82**, 041914.
59. E. M. Furst and T. M. Squires, *Microrheology*, 2017, DOI: 10.1093/oso/9780199655205.001.
60. K. Joyner, S. Yang and G. A. Duncan, *Apl Bioengineering*, 2020, **4**.
61. S. S. Rogers, C. van der Walle and T. A. Waigh, *Langmuir*, 2008, **24**, 13549-13555.
62. A. Kowalczyk, C. Oelschlaeger and N. Willenbacher, *Meas Sci Technol*, 2015, **26**.
63. B. Rosner and D. Grove, *Stat Med*, 1999, **18**, 1387-1400.
64. Y. H. Zhou, Y. Y. Zhu and W. K. Wong, *Cont Clin Trial Comm*, 2023, **33**.
65. M. Wells, M. Mikesh and V. Gordon, *J Microsc-Oxford*, 2024, **293**, 59-68.
66. W. Z. Liu, H. L. Roder, J. S. Madsen, T. Bjarnsholt, S. J. Sorensen and M. Burmolle, *Frontiers in Microbiology*, 2016, **7**.
67. W. Z. Liu, S. Jacquiod, A. Brejnrod, J. Russel, M. Burmolle and S. J. Sorensen, *Isme Journal*, 2019, **13**, 3054-3066.
68. S. C. Booth and S. A. Rice, *Biofilm*, 2020, **2**.
69. L. Eigentler, F. A. Davidson and N. R. Stanley-Wall, *Open Biol*, 2022, **12**.
70. P. Herman-Bausier, C. Valotteau, G. Pietrocola, S. Rindi, D. Alsteens, T. J. Foster, P. Speziale and Y. F. Dufrene, *mBio*, 2016, **7**.
71. A. Madani, K. Garakani and M. R. K. Mofrad, *PLoS One*, 2017, **12**, e0179601.
72. M. C. Hudson, W. K. Ramp and K. P. Frankenburg, *FEMS Microbiol Lett*, 1999, **173**, 279-284.
73. M. O. Elasri, J. R. Thomas, R. A. Skinner, J. S. Blevins, K. E. Beenken, C. L. Nelson and M. S. Smeltzer, *Bone*, 2002, **30**, 275-280.
74. Y. Iwata, K. Satou, K. Furuichi, I. Yoneda, T. Matsumura, M. Yutani, Y. Fujinaga, A. Hase, H. Morita, T. Ohta, Y. Senda, Y. Sakai-Takemori, T. Wada, S. Fujita, T. Miyake, H. Yasuda, N. Sakai, S. Kitajima, T. Toyama, Y. Shinozaki, A. Sagara, T. Miyagawa, A. Hara, M. Shimizu, Y. Kamikawa, K. Ikeo, S. Shichino, S. Ueha, T. Nakajima, K. Matsushima, S. Kaneko and T. Wada, *Int J Infect Dis*, 2020, **91**, 22-31.
75. S. Kadam, S. Nadkarni, J. Lele, S. Sakhalkar, P. Mokashi and K. S. Kaushik, *Front Bioeng Biotech*, 2019, **7**.

TEXAS TECH UNIVERSITY
Edward E. Whitacre Jr.
College *of* Engineering™

Department of Mechanical Engineering

All data for this paper will be made available on the TTU instance of the Texas Data Repository.

Box 41021 | Lubbock, Texas 79409-1021 | T 806.742.3563 | F 806.742.3540
An EEO/Affirmative Action Institution